Examination of Multiple Spectral Exponents of Epileptic ECoG Signal

Suparerk Janjarasjitt *Member, IAENG,* and Kenneth A. Loparo

***Abstract*—In this paper, the wavelet-based fractal analysis is applied to analyze an electrocorticogram (ECoG) signal recorded from an epilepsy patient. A spectral exponent γ yielded from the wavelet-based fractal analysis is determined from a slope of $\log_2 \mathrm{var}(d_{m,n})$-$m$ graph over an interval of levels. Rather than a single spectral exponent, multiple spectral exponents determined from various intervals of levels corresponding to various ranges of spectral subbands of the ECoG signal are examined. From the computational results, it is observed that the spectral exponents of the ECoG signal estimated from different intervals of levels m exhibit different intriguing characteristics. It is also shown that the spectral exponents of the ECoG signal obtained during epileptic seizure events are significantly different from those of the ECoG signal obtained during non-seizure period. Furthermore, during non-seizure period the spectral exponent of the ECoG signal tends to decrease as the corresponding range of frequencies of subband decreases. On the contrary, for almost all spectral subbands the spectral exponents of the ECoG signal tend to be comparable except the lowest frequency subband.**

***Index Terms*—wavelet analysis, fractals, epilepsy, seizure, electrocorticogram**

I. Introduction

Epilepsy is a common brain disorder in which clusters of neurons signal abnormally [1]. About 50 million people have epilepsy worldwide [2]. Epileptic seizures are manifestations of epilepsy [3]. Electroencephalogram (EEG), a signal that quantifies the electrical activity of the brain, is commonly used to assess behaviors of the brain and also detect abnormalities of the brain. The EEG is also crucial for the fundamental diagnosis of epilepsy [1]. EEGs are typically recorded using electrodes placed on the scalp. A scalp EEG is however very sensitive to signal attenuation and artifacts, and has poor spatial resolution. An intracranial EEG or an electrocorticogram (ECoG) is an alternative approach to measure the electrical activity of the brain by placing electrodes on the cortex.

Concepts and computational tools derived from the study of complex systems including nonlinear dynamics and fractals gained increasing interest for applications in biology and medicine [4]. One of the reasons is that physiological signals and systems can exhibit an extraordinary range of patterns and behaviors [4]. Furthermore, there is evidence that some biological systems can exhibit scale-invariant or scale-free behavior, in the sense that they do not have a characteristic length or time scale that dominates the dynamics of the underlying process [5]–[7].

S. Janjarasjitt is with the Department of Electrical and Electronic Engineering, Ubon Ratchathani University, Ubon Ratchathani, 34190 Thailand e-mail: ensupajt@ubu.ac.th.

K. A. Loparo is with the Department of Electrical Engineering and Computer Science, Case Western Reserve University, Cleveland, OH, 44106 USA.

The mathematical concept of a fractal is commonly associated with irregular objects that exhibit a geometric property called scale-invariance or self-similarity [4], [8]. Fractal forms are composed of subunits resembling the structure of the macroscopic object [4] which in nature can emerge from statistical scaling behavior in the underlying physical phenomena [9]. Many physical, biological or physiological signals may however not exhibit just a simple monofractal scaling behavior [10]. These multifractal signals are associated with different self-similar behaviors on various scales ranging from small to large scales.

The wavelet transform is a natural tool for characterizing scale-invariant or self-similar signals and plays a significant role in the study of self-similar signals and systems [9], in particular $1/f$ processes [9], [11]. In [11], a wavelet-based representation for $1/f$ processess was developed where the spectral exponent γ is determined from the slope of the $\log_2$-var of wavelet-coefficients versus the level. The spectral exponent specifies the distribution of power from low to high frequencies. The spectral exponent is directly related to self-similar parameter [12], and also can be used for long-range correlation characterization [13]. The wavelet-based approach [11] has been widely applied to examine the scale-invariant characteristics of epileptic EEG/ECoG data associated with various states of the brain [14]–[16] and also compared to the other common measures including the correlation dimension [17] and the Hurst exponents [18], [19].

Typically, a single spectral exponent determined from a specific interval of levels of epileptic EEG/ECoG data is examined. In [20], multiple spectral exponents determined from various intervals of levels (or ranges of spectral subbands) of the epileptic ECoG epochs. It was shown that the epileptic ECoG epochs are associated with different spectral exponents depending on the interval of levels they are determined from. This suggests that the epileptic ECoG epochs are associated with different self-similar behaviors on various scales. In this paper, the study is extended to examine characteristics of multiple spectral exponents of long-term continuous ECoG data determined from various intervals of levels.

II. Materials and Methods

A. ECoG Data

Long-term ECoG data of an epilepsy patient at University Hospitals of Cleveland, Case Medical Center in Cleveland, Ohio, USA are analyzed. With the consent of the patient, the long-term ECoG data were recorded using a Nihon-Kohden EEG system (band-pass (0.10–300 Hz) filter, 1,000 Hz sampling rate) prior to surgery. A 6-hour segment of single-channel ECoG data examined is acquired from within the focal region of epileptic seizures. This ECoG segment

(Advance online publication: 23 August 2014)

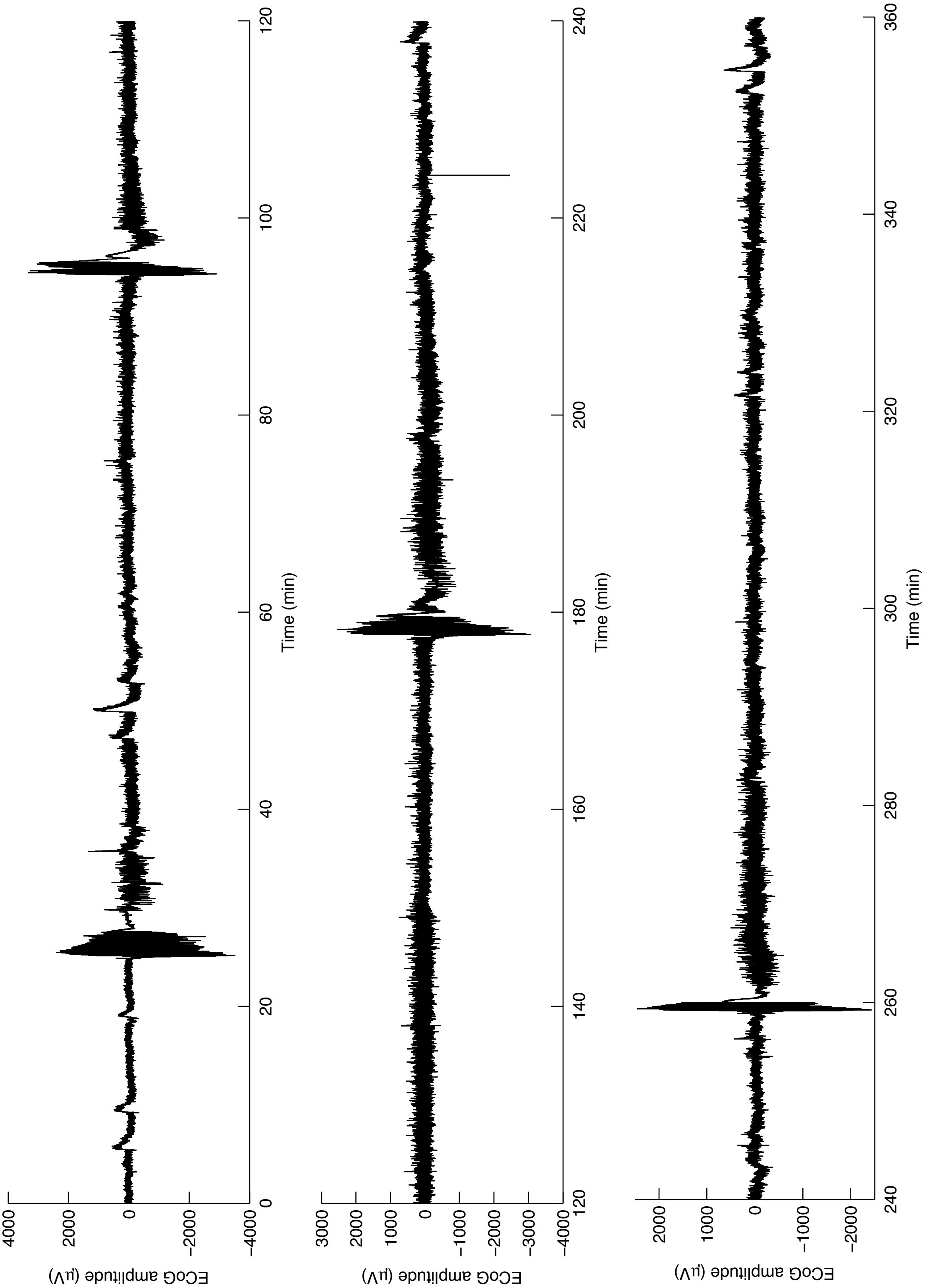

Fig. 1. The 6-hour segment of single-channel ECoG data examined.

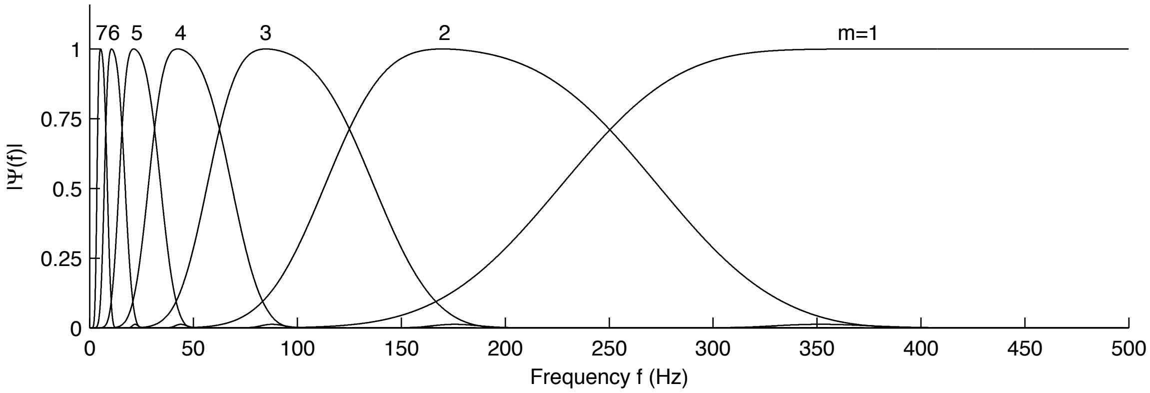

Fig. 2. The corresponding spectral subbands of the 10th order of Daubechies wavelets at the levels $m = 1, 2, \ldots, 7$.

contains four epileptic seizure events occurring between 24m 47s and 27m 36s, 1h 33m 57s and 1h 25m 45s, 2h 57m 19s and 3h 2m 11s, and 4h 18m 50s and 4h 20m 1s. The ECoG signal is shown in Fig. 1. In general, both magnitude and pattern of the ECoG signal change significantly during epileptic seizure events.

B. Wavelet-Based Fractal Analysis

Models of $1/f$ processes are generally represented using a frequency-domain characterization. The dynamics of $1/f$ processes exhibit power-law behaviors [21] and can be characterized in the form of [11]

$$S_x(\omega) \sim \frac{\sigma_x^2}{|\omega|^\gamma} \tag{1}$$

over several decades of the frequency ω, where $S_x(\omega)$ is the Fourier transform of the signal $x(t)$ and γ denotes the spectral exponent.

In [11], [22], it was proved that a random process $x(t)$ constructed by the wavelet basis expansions

$$x(t) = \sum_m \sum_n d_{m,n} \psi_{m,n}(t) \tag{2}$$

where $\psi_{m,n}(t)$ is an orthonormal wavelet basis and $d_{m,n}$ are the wavelet coefficients has a time-averaged spectrum

$$S_x(\omega) = \sigma^2 \sum_m 2^{-\gamma m} \left|\Psi\left(2^{-m}\omega\right)\right|^2 \tag{3}$$

that is nearly-$1/f$, i.e.,

$$\frac{\sigma_L^2}{|\omega|^\gamma} \leq X(\omega) \leq \frac{\sigma_U^2}{|\omega|^\gamma} \tag{4}$$

for some $0 < \sigma_L^2 \leq \sigma_U^2 < \infty$. Variances of the wavelet coefficients $d_{m,n}$ that are a collection of mutually uncorrelated, zero-mean random variables are

$$\mathrm{var}(d_{m,n}) = \sigma^2 2^{-\gamma m}. \tag{5}$$

The spectral exponent γ of a $1/f$ process can therefore be determined from the linear relationship between $\log_2\ \mathrm{var}(d_{m,n})$ and levels m, i.e.,

$$\gamma = \frac{\Delta \log_2\ \mathrm{var}(d_{m,n})}{\Delta m}. \tag{6}$$

The steps for computing the spectral exponent γ of the time series x using the wavelet-based fractal analysis are as follows [20]:

1) Decompose an ECoG epoch into M levels using the wavelet-basis expansions to obtain the wavelet coefficients $d_{m,n}$ where levels $m = 1, 2, \ldots, M$.
2) Compute the variance of wavelet coefficients $d_{m,n}$ corresponding to each level m, $\mathrm{var}(d_{m,n})$.
3) Take the logarithm to base 2 of the corresponding variances of wavelet coefficients, $\log_2 \mathrm{var}(d_{m,n})$.
4) Compute the spectral exponent γ by estimating the slope of a $\log_2 \mathrm{var}(d_{m,n})$-$m$ graph between the specified levels m.

C. Analytic Framework

In the computational experiment, the ECoG signal is partitioned into 5-second epochs without overlapping segments. The state of the brain the ECoG epochs are associated with is divided into two states: during non-epileptic seizure period and during epileptic seizure event. The epochs of ECoG signal are decomposed into seven levels using the 10th order of Daubechies wavelet (Db10). The spectral subbands corresponding to the levels $m = 1, 2, \ldots, 7$ range approximately between 250.00–500.00 Hz, 125.00–250.00 Hz, 62.50–125.00 Hz, 31.25–62.50 Hz, 15.63–31.25 Hz, 7.81–15.63 Hz, and 3.91–7.81 Hz, respectively. The spectral subbands of the 10th order of Daubechies wavelet corresponding to levels $m = 1, 2, \ldots, 7$ are shown in Fig. 2.

The spectral exponents of ECoG epochs are estimated using a linear least-squares regression technique from five intervals of levels referred to as intervals L_1, L_2, L_3, L_4, and L_5: $m = 1, 2, 3$, $m = 2, 3, 4$, $m = 3, 4, 5$, $m = 4, 5, 6$, and $m = 5, 6, 7$, respectively. The spectral exponents determined from the intervals L_1, L_2, L_3, L_4, and L_5 are, respectively, referred to as γ_1, γ_2, γ_3, γ_4, and γ_5.

III. Results

The spectral exponents γ_1, γ_2, γ_3, γ_4 and γ_5 of the first, second, and last 2-hour segments of the ECoG signal are shown in Figs. 3(a)–(e), Figs. 4(a)–(e), and Figs. 5, respectively. In addition, the spectral exponents γ_1, γ_2, γ_3, γ_4, and γ_5 of the ECoG signal are illustrated as a color-map plot in Fig. 6. The color bar indicates the magnitude of spectral exponent where the black and the white colors

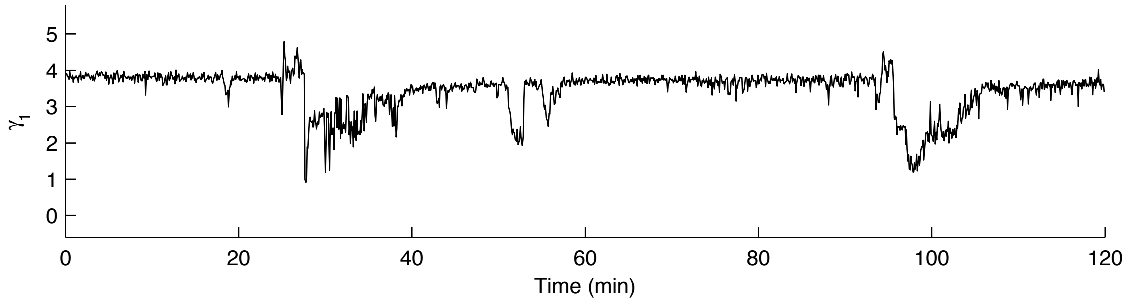

(a) γ_1

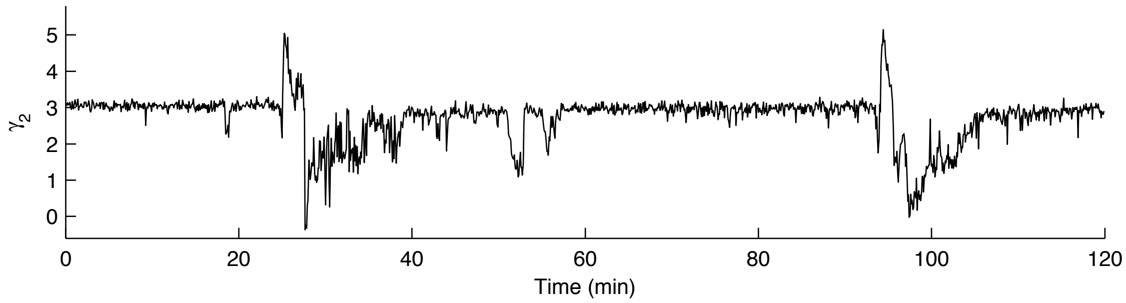

(b) γ_2

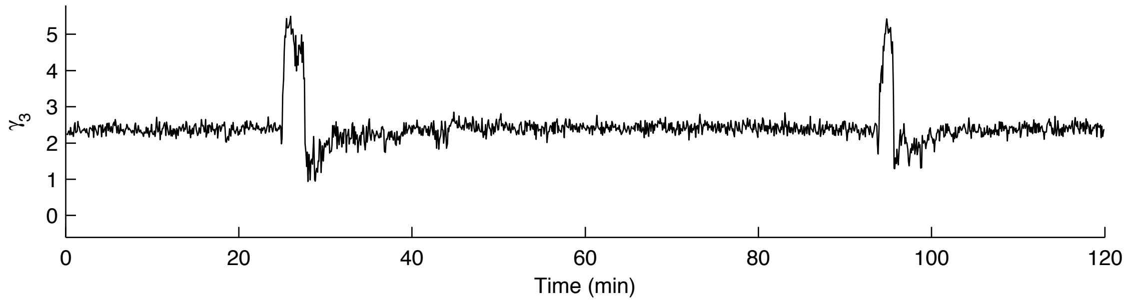

(c) γ_3

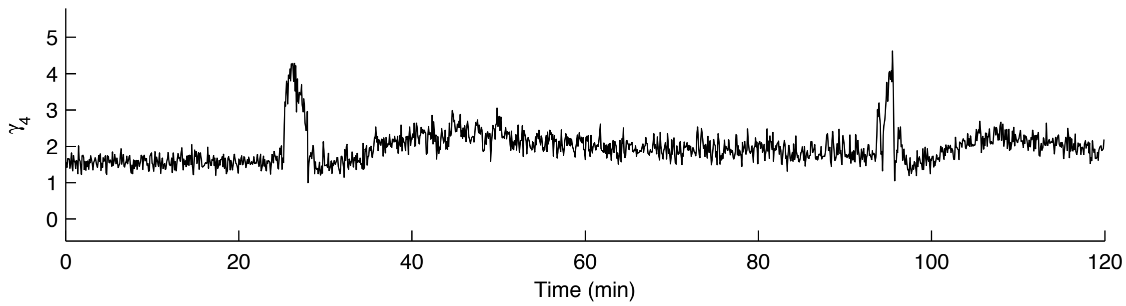

(d) γ_4

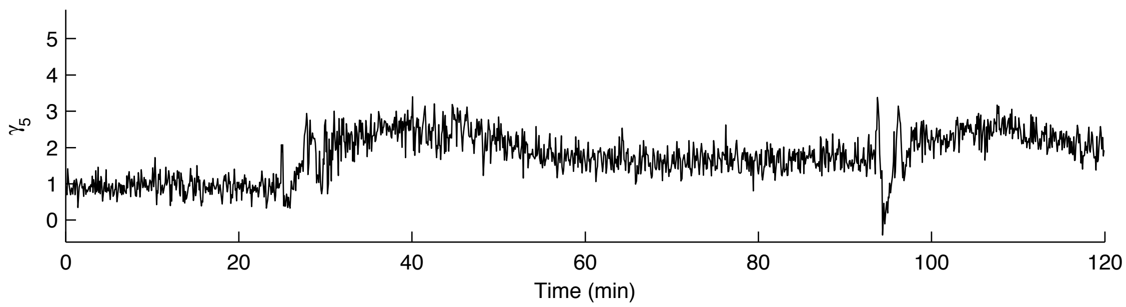

(e) γ_5

Fig. 3. The corresponding spectral exponents of the first 2-hour segment of the ECoG signal determined from various intervals of levels.

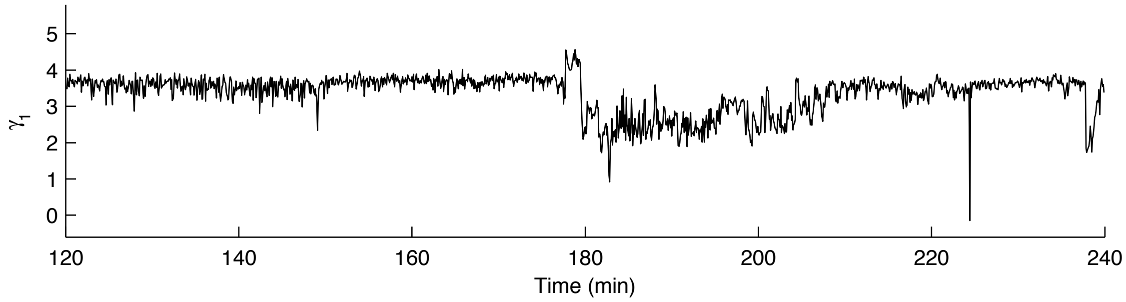

(a) γ_1

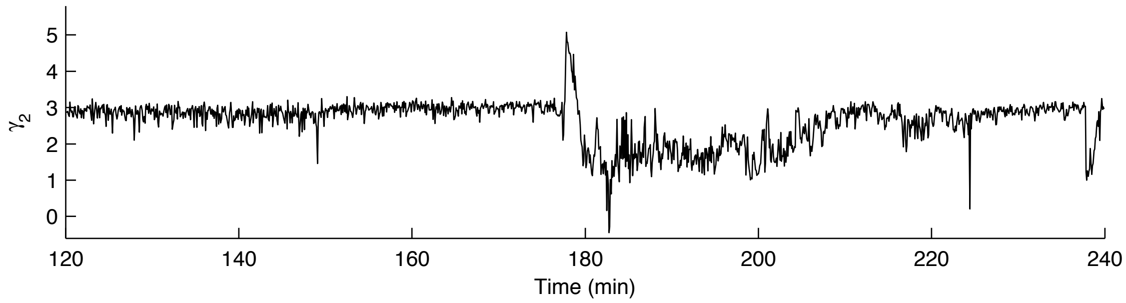

(b) γ_2

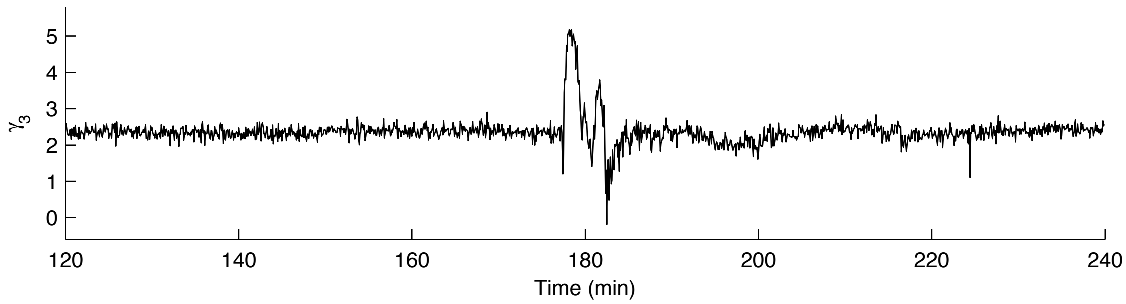

(c) γ_3

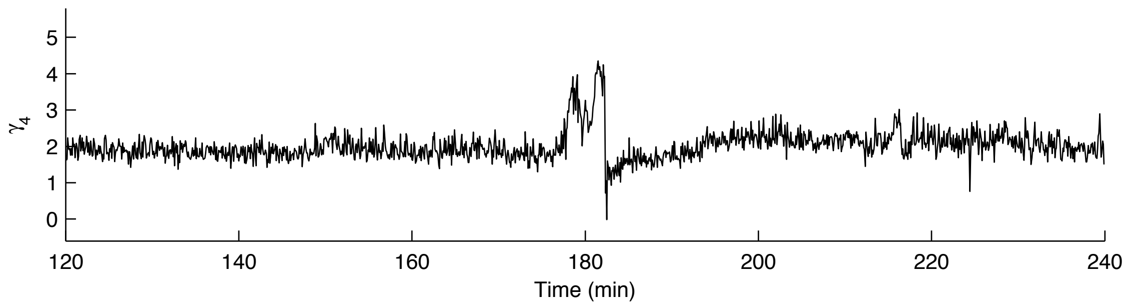

(d) γ_4

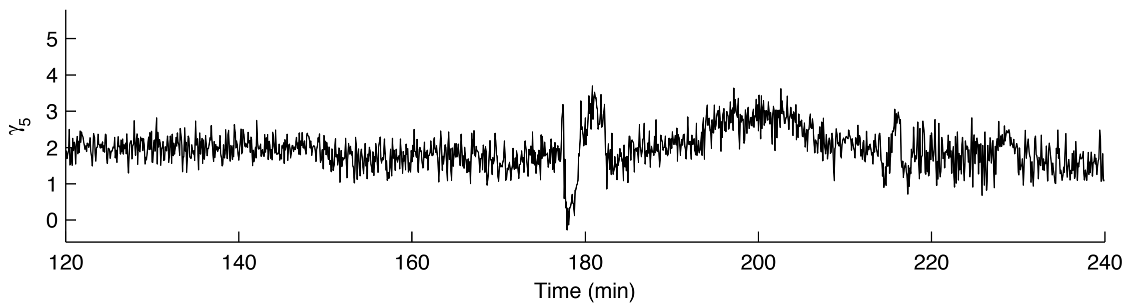

(e) γ_5

Fig. 4. The corresponding spectral exponents of the second 2-hour segment of the ECoG signal determined from various intervals of levels.

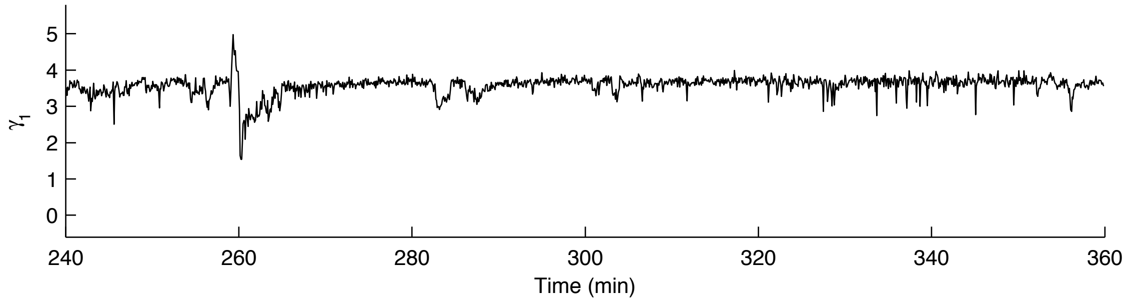

(a) γ_1

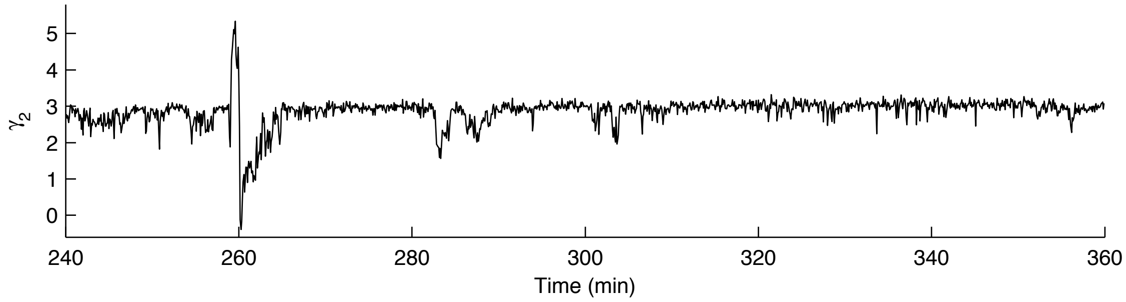

(b) γ_2

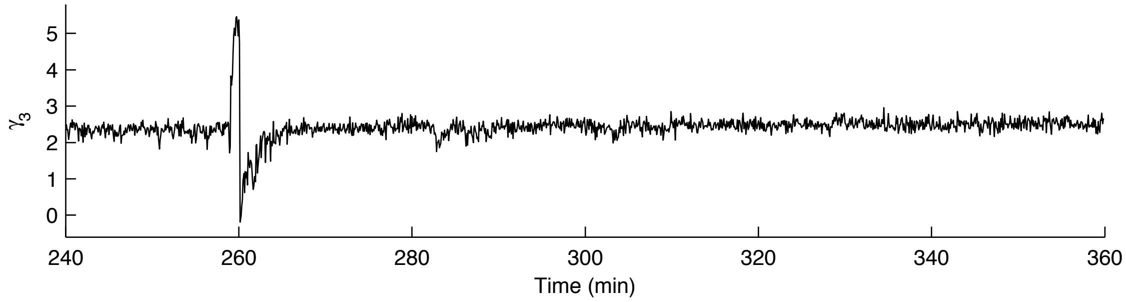

(c) γ_3

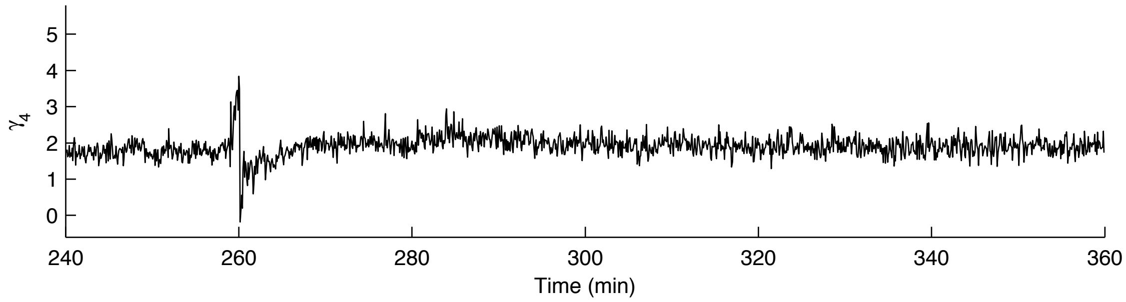

(d) γ_4

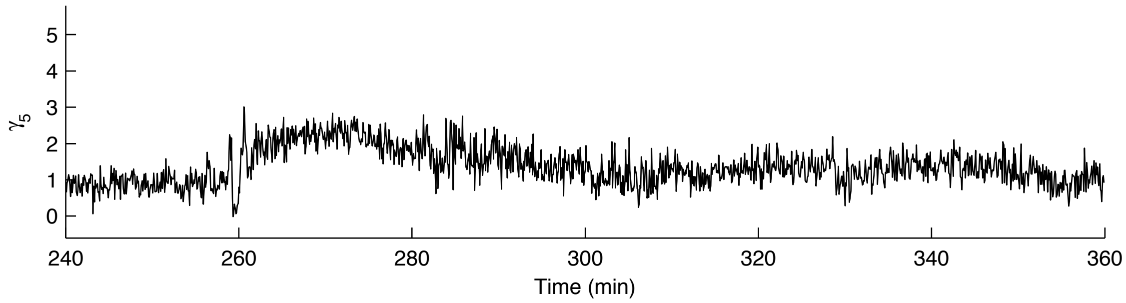

(e) γ_5

Fig. 5. The corresponding spectral exponents of the last 2-hour segment of the ECoG signal determined from various intervals of levels.

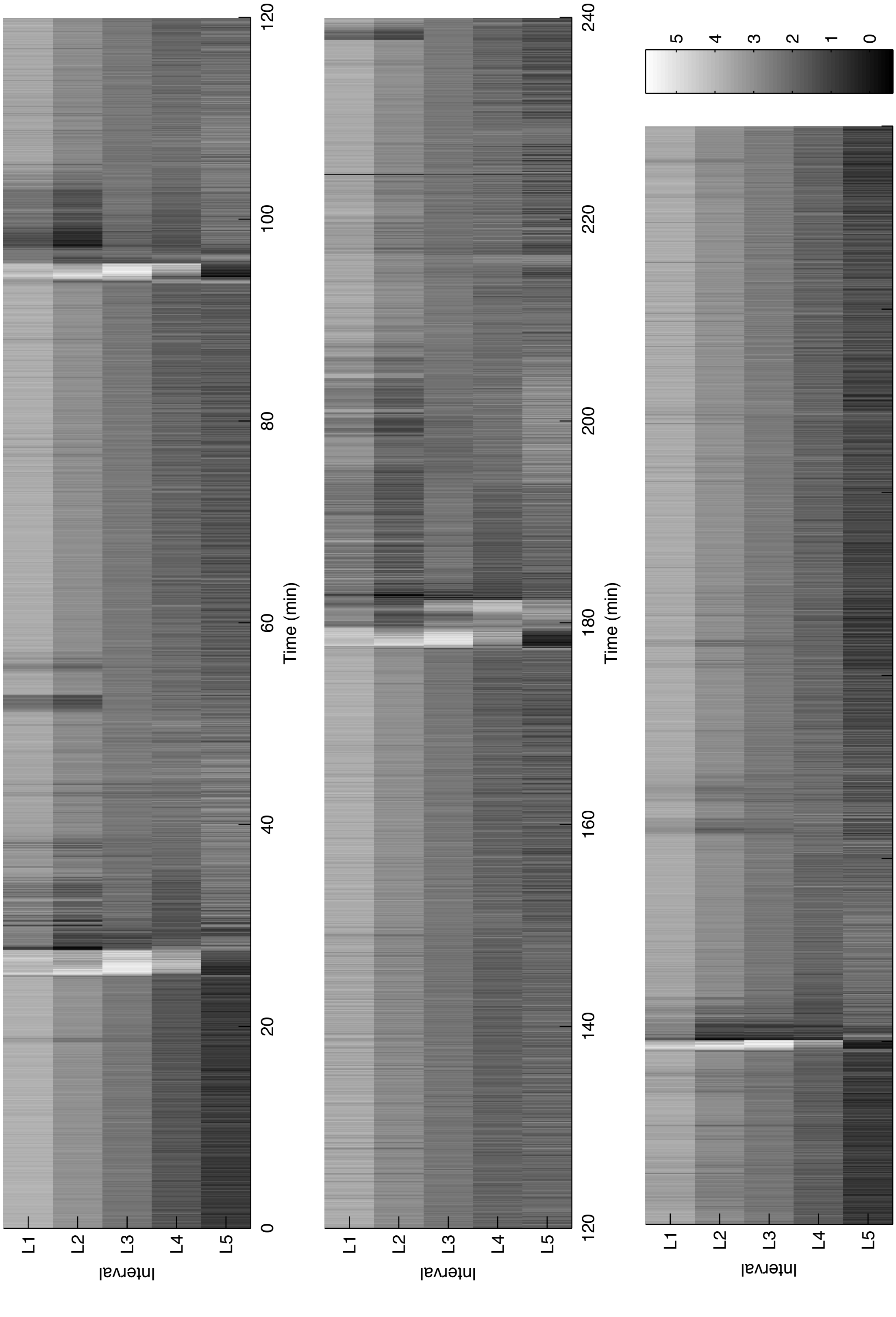

Fig. 6. The color-map plot of the spectral exponents of the ECoG signal determined from various intervals of levels.

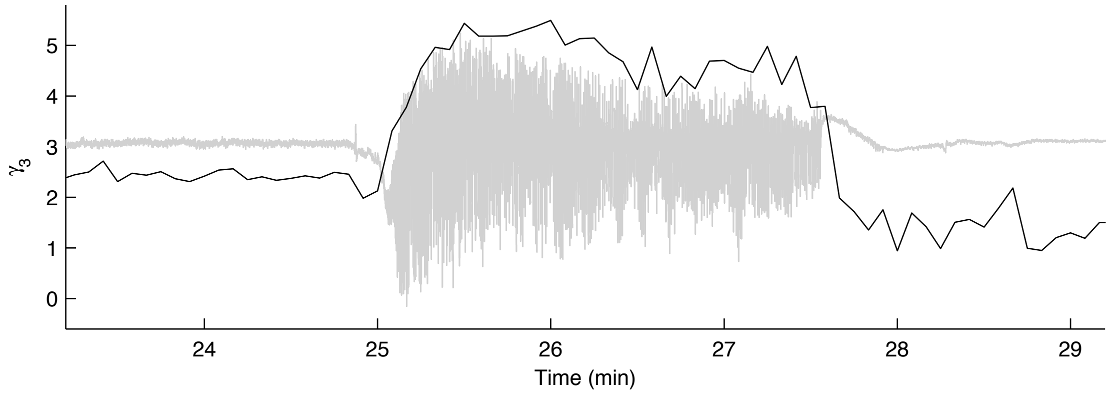

(a) Seizure 1

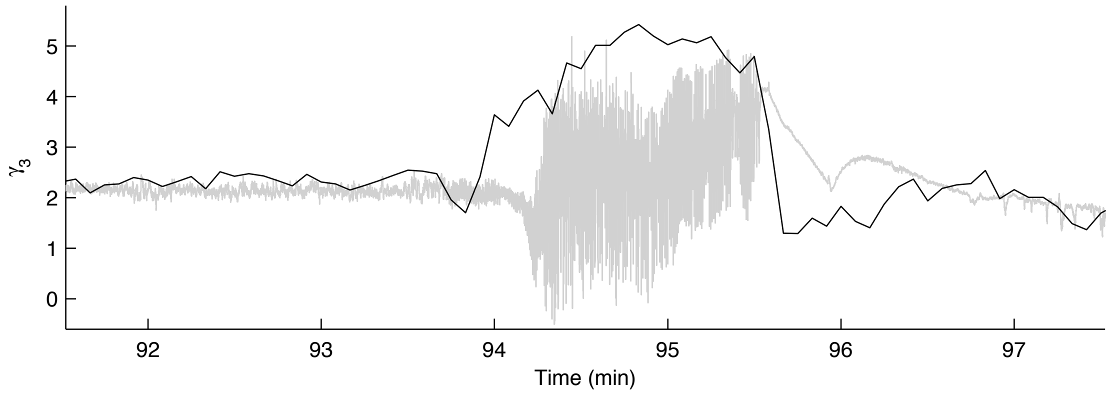

(b) Seizure 2

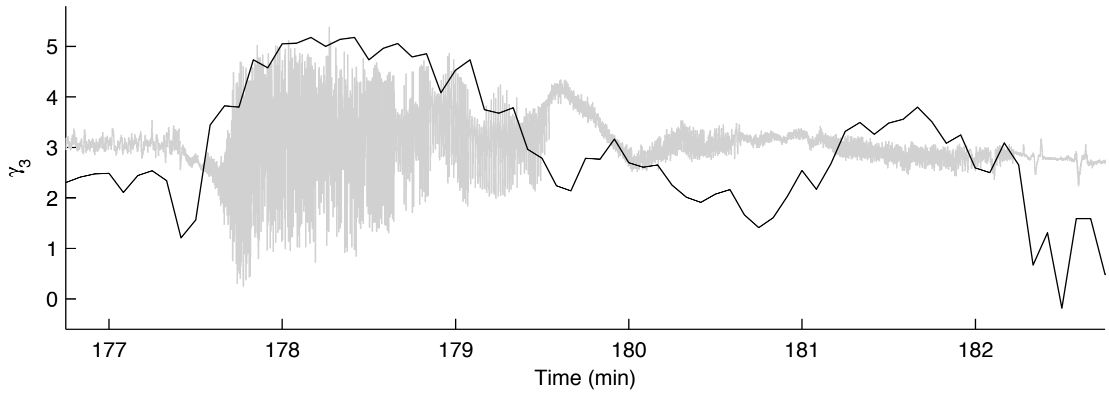

(c) Seizure 3

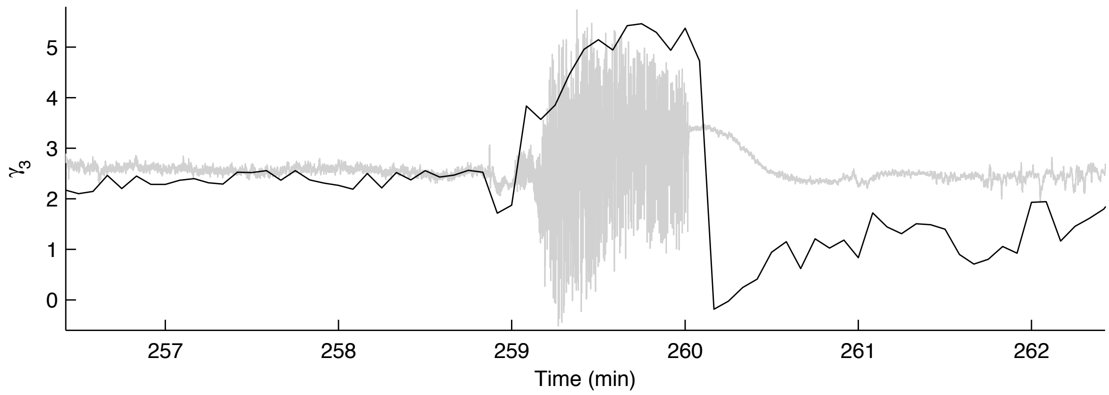

(d) Seizure 4

Fig. 7. The spectral exponents of the ECoG signal around the corresponding epileptic seizure events.

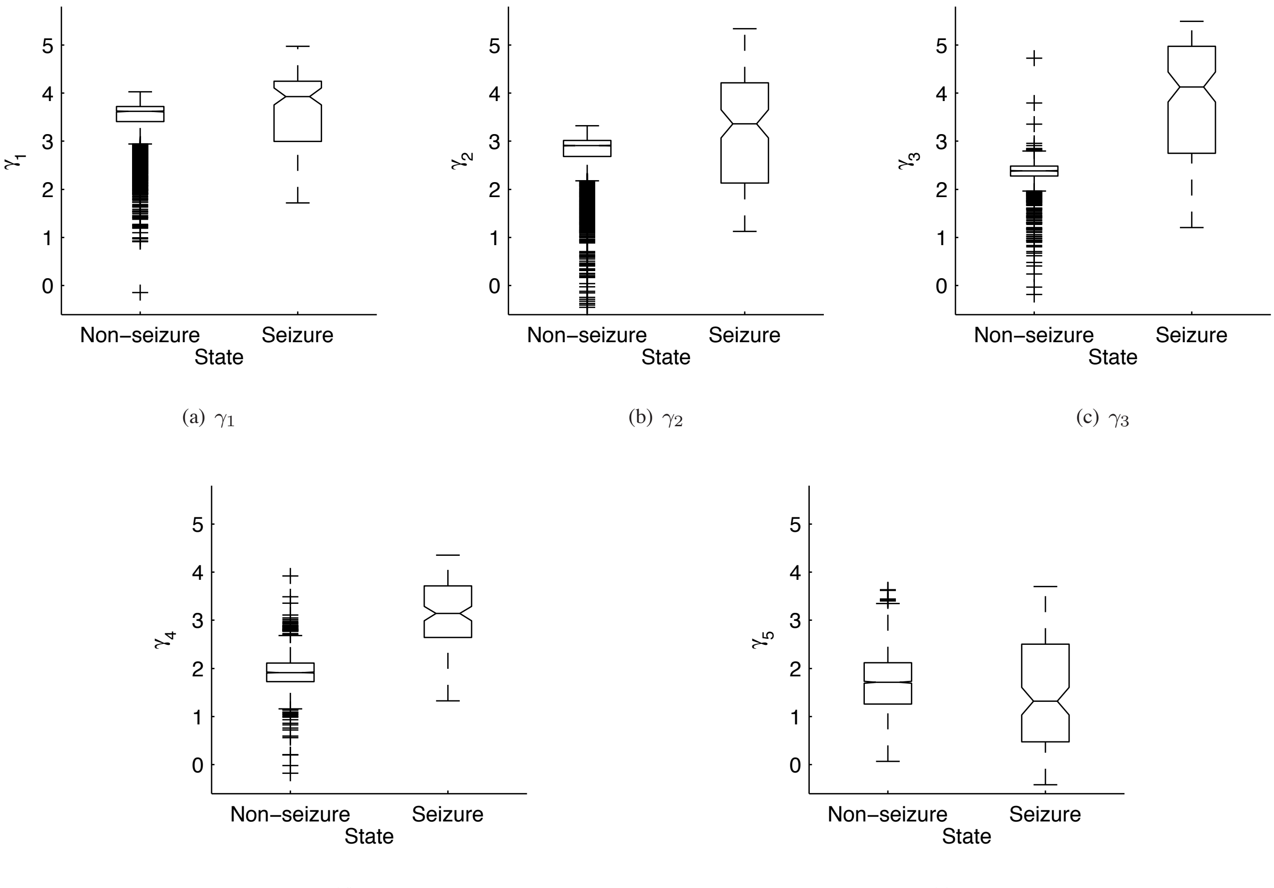

(a) γ_1 (b) γ_2 (c) γ_3 (d) γ_4 (e) γ_5

Fig. 8. Comparison of the spectral exponents of the ECoG signal obtained during non-epileptic seizure period and epileptic seizure events.

denote the spectral exponents of -0.6 and 5.8, respectively. In general, the spectral exponents γ_1, γ_2, γ_3, and γ_4 of the ECoG signal tend to dramatically increase from the baseline during epileptic seizure events while the spectral exponent γ_5 of the ECoG signal tend to slightly decrease from the baseline during epileptic seizure event.

The most intriguing characteristic of spectral exponents of the ECoG signal obtained during epileptic seizure events is observed at the interval L_3. Further, in Figs. 7(a)–(d), the spectral exponents γ_3 (plotted in black) around the first, second, third, and last epileptic seizure events are compared to the corresponding ECoG signal (plotted in gray), respectively. Evidently, the significant changes of spectral exponent γ_3 of the ECoG signal occur about the beginning and the end of epileptic seizure events.

Box plots shown in Fig. 8(a)–(e) compares the spectral exponents of the ECoG epochs obtained during non-seizure period and epileptic seizure events determined from intervals L_1, L_2, L_3, L_4, and L_5, respectively. It is shown that the spectral exponents γ_1, γ_2, γ_3, and γ_4 of the ECoG epochs obtained during epileptic seizure events tend to be higher than those of the ECoG epochs obtained during non-seizure period. On the contrary, the spectral exponents γ_5 of the ECoG epochs obtained during epileptic seizure events tend to be lower than those of the ECoG epochs obtained during non-seizure period.

In addition, the spectral exponents γ_1, γ_2, γ_3, γ_4, and γ_5 of the ECoG signal obtained during non-seizure period and epileptic seizure events are compared in box plots shown in Fig. 9(a)–(b), respectively. It is shown that the characteristics of the spectral exponents γ_1, γ_2, γ_3, γ_4, and γ_5 of the ECoG signal obtained during non-seizure period and epileptic seizure events are remarkably different. The means and the standard deviations of the spectral exponents of the ECoG epochs obtained during non-seizure period and epileptic seizure events are summarized in Table I.

IV. Discussion

The computational results show that the spectral exponents of the ECoG signal vary according to the state of the brain and also the interval of levels (ranges of spectral subbands) from which the spectral exponents are determined. In general, the spectral exponents determined from higher frequency subbands (62.50–500.00Hz, 31.25–250.00Hz, 15.63–125.00Hz, and 7.81–62.50Hz subbands) of the ECoG signal exhibit similar characteristics while the characteristic of the spectral exponent determined from the lowest frequency subband (3.91–31.25Hz subband) is completely different from the others. During epileptic seizure events the spectral exponents determined from 62.50–500.00Hz, 31.25–250.00Hz, 15.63–125.00Hz, and 7.81–62.50Hz subbands of the ECoG signal tend to be higher but the spectral exponent determined from the 3.91–31.25Hz subband of the ECoG signal tend to be lower compared to the baseline of the corresponding spectral exponents.

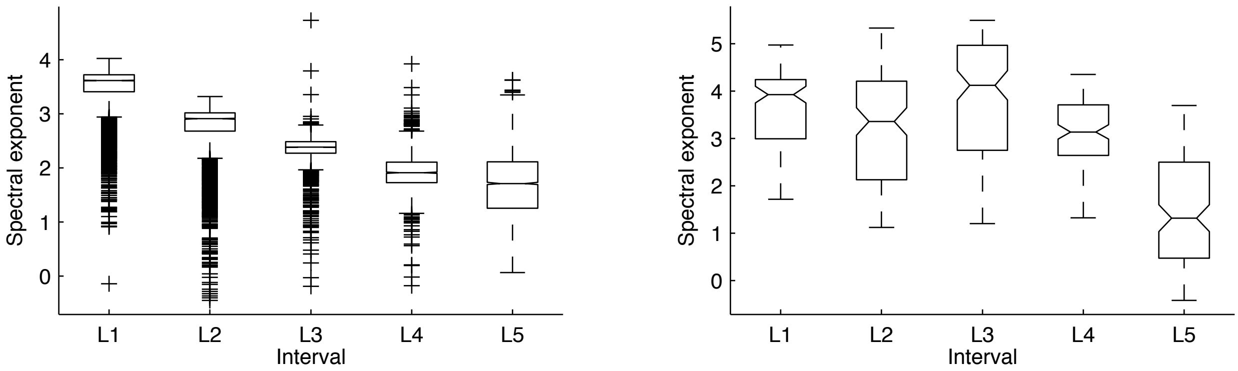

(a) Non-seizure period

(b) Epileptic seizure event

Fig. 9. Comparison of the spectral exponents of the ECoG signal determined from intervals L_1, L_2, L_3, L_4, and L_5.

TABLE I
STATISTICAL VALUES (MEAN±S.D.) OF THE SPECTRAL EXPONENTS OF THE ECOG SIGNALS OBTAINED DURING NON-SEIZURE PERIOD AND EPILEPTIC SEIZURE EVENTS.

Interval	State	
	Non-seizure	Seizure
L_1	3.4605±0.4565	3.6405±0.7511
L_2	2.7238±0.5162	3.2396±1.1769
L_3	2.3560±0.2405	3.8697±1.2158
L_4	1.9226±0.3050	3.0966±0.7494
L_5	1.7028±0.5911	1.4898±1.1125

In addition, the spectral exponents determined from the highest frequency subbands (62.50–500.00Hz and 31.25–250.00Hz subbands) exhibit another intriguing characteristic after the end of epileptic seizure events. At those subbands there are substantial decrease in the spectral exponents of the ECoG signal right after the end of epileptic seizure events before the spectral exponents gradually increases returning to the baseline. The spectral exponent determined from the 15.26–125.00Hz subband of the ECoG signal clearly manifests epileptic seizure events. This also suggests that the beginning and the end of epileptic seizure events can be identified.

During non-seizure period, the spectral exponent tends to decrease as the corresponding range of frequencies of subband of the ECoG signal decreases. That is, the spectral exponent determined from the 62.50–500.00Hz subband of the ECoG signal tends to be higher than that determined from the 31.25–250.00Hz subband of the ECoG signal that is higher than that determined from the 15.63–125.00Hz subband of the ECoG signal, and so on. However, during epileptic seizure events, the spectral exponents determine from various spectral subbands of the ECoG signal tend to be comparable except the spectral exponent determined from the 3.91–31.25Hz subband that tends to be lower than the others.

V. CONCLUSIONS

In this paper, it is evidenced that the spectral exponent of the ECoG signal varies according to the state of the brain and also exhibits distinguishable characteristics of epileptic seizure events regardless of the spectral subband of the ECoG signal. Furthermore, the spectral exponents determined from different spectral subbands of the ECoG signal obtained from the same state of the brain, i.e, non-seizure period and epileptic seizure event, exhibit distinctive characteristics. These remarkable characteristics of the spectral exponents of the ECoG signal can be further applied for epileptic seizure detection.

REFERENCES

[1] Seizure and Epilepsy: Hope through Research National Institute of Neurological Disorders and Stroke (NINDS), Bethesda, MD, 2004 [Online]. Available: http://www.ninds.nih.gov/disorders/epilepsy/detail_epilepsy.htm

[2] Z. Kovacs and A. Dobolyi, "Epilepsy and its therapy: present and future," *Current Medicinal Chemistry*, vol. 21, pp. 651, 2014.

[3] A. Subasi, "Epileptic seizure detection using dynamic wavelet network," *Expert Systems with Applications*, vol. 29, pp. 343–355, 2005.

[4] A. L. Goldberger, "Complex systems," *Proc. Am. Thorac. Soc.*, vol. 3, pp. 467–472, 2006.

[5] S. Havlin, S. V. Buldyrev, A. L. Goldberger, R. N. Mantegna, S. M. Ossadnik, C.-K. Peng, M. Simons and H. Stanley, "Fractals in biology and medicine," *Chaos, Solitons & Fractals*, vol. 6, pp. 171–201, 1995.

[6] C. J. Stam and E. A. de Bruin, "Scale-free dynamics of global functional connectivity in the human brain," *Human Brain Mapping*, vol. 22, pp. 97–109, 2004.

[7] K. Linkenkaer-Hansen, V. V. Nikouline, J. M. Palva and R. J. Ilmoniemi, "Long-range temporal correlations and scaling behavior in human brain oscillations," *J. Neurosci.*, vol. 21, pp. 1370–1377, 2001.

[8] B. B. Mandelbrot, *The Fractal Geometry of Nature*, San Francisco: WH Freeman, 1982.

[9] G. W. Wornell, *Signal Processing with Fractals: A Wavelet-Based Approach*, New Jersey: Prentice Hall, 1995.

[10] J. W. Kantelhardt, S. A. Zschiegner, E. Koscielny-Bunde, S. Havlin, A. Bunde and H. E. Stanley, "Multifractal detrended fluctuation analysis of nonstationary time series," *Physica A*, vol. 316, pp. 87–114, 2002.

[11] G. W. Wornell, "Wavelet-based representations for the $1/f$ family of fractal processes," *Proceedings of the IEEE*, vol. 81, pp. 1428–1450, 1993.

[12] A. L. Goldberger, L. A. N. Amaral, J. M. Hausdorff, P. Ch. Ivanov, C.-K. Peng and H. E. Stanley, "Fractal dynamics in physiology: alterations with disease and aging," *PNAS*, vol. 99, pp. 2466-2472, 2002.

[13] S. Janjarasitt, "Computational validation of fractal characterization by using the wavelet-based fractal analysis," *J. Korean Phys. Soc.*, vol. 64, pp. 780–785, 2014.

[14] S. Janjarasjitt and K. A. Loparo, "Examination of scale-invariant characteristics of multi-channel ECoG data for epileptic seizure localization," *J. Med. Biol. Eng.*, doi: 10.5405/jmbe.1692.

[15] S. Janjarasjitt and K. A. Loparo, "Wavelet-based fractal analysis of multi-channel epileptic ECoG," in *Proc. TENCON*, 2010, pp. 373–378.

[16] S. Janjarasjitt and K. A. Loparo, “Wavelet-based fractal analysis of the epileptic EEG signal,” in *Proc. ISPACS*, 2009, pp. 127–130.

[17] S. Janjarasjitt and K. A. Loparo, “Comparison of complexity measures using two complex system analysis methods applied to the epileptic ECoG,” *J. Korean Phys. Soc.*, vol. 63, pp. 1659–1665, 2013.

[18] S. Janjarasjitt and K. A. Loparo, “Examination of scale-invariant characteristics of epileptic electroencephalograms using wavelet-based analysis,” *Computers and Electrical Engineering*, vol. 40, pp. 1766-1773.

[19] S. Janjarasjitt and K. A. Loparo, “Scale-invariant behavior of epileptic ECoG,” *J. Med. Biol. Eng.*, doi: 10.5405/jmbe.1433.

[20] S. Janjarasjitt and K. A. Loparo, “Characteristic of spectral exponent of epileptic ECoG data corresponding to levels in wavelet-based fractal analysis,” Lecture Notes in Engineering and Computer Science: Proceedings of The International MultiConference of Engineers and Computer Scientists 2014, IMECS 2014, 12-14 March, 2014, Hong Kong, pp. 140–143.

[21] P. A. Watters, “Fractal structure in the electroencephalogram,” *Complexity International*, vol. 5, 1998.

[22] G. W. Wornell, “Synthesis, analysis, and processing of fractal signals,” Ph.D. Thesis, Massachusetts Institute of Technology, Massachusetts, U.S.A., 1991.